Magnesium Technology 2012
Edited by: Suveen N. Mathaudhu, Wim H. Sillekens, Neale R. Neelameggham, and Norbert Hort
TMS (The Minerals, Metals & Materials Society), 2012

SLIDING WEAR BEHAVIOUR OF SQUEEZE CAST MAGNESIUM COMPOSITE AM60-9% $(Al_2O_3)_f$

A. Banerji[1], H. Hu[1], A.T. Alpas[1]

[1]Department of Mechanical, Automotive & Materials Engineering,
University of Windsor, 401 Sunset Avenue,
Windsor, Ontario, Canada N9B 3P4

Keywords: Squeeze cast composites, Sliding wear, Wear loss of alloy and composites, Damage to counterface

Abstract

Magnesium matrix (AM60) composites reinforced with 9 vol% Al_2O_3 fibres were fabricated using Al_2O_3fibre preform preparation and squeeze casting techniques. Boundary lubricated sliding wear tests were performed on the composites and the matrix alloy at low loads (1.0-5.0 N) to evaluate their wear characteristics. The Mg matrix alloy underwent scuffing and oxidative type wear leading to high rate of material removal. Under the same conditions, the composites' wear resistance was at least 10^2 times higher. At 1.0 N load, Al_2O_3fibres protected the matrix from damage for up to 1.0×10^6 sliding cycles. For longer cycles Al_2O_3 fibres underwent fracture and exhibited decohesion at the fibre/matrix interface. At higher loads and sliding cycles, the matrix suffered wear damage leading to an increase in wear rate. The counterface, AISI 52100, worn against the base alloy AM60 revealed slight damage in the form of surface scratches and presence of MgO. The counterface experienced higher amount of material removal when it was worn against AM60-9% $(Al_2O_3)_f$ composite.

Introduction

During the last two decades, automotive engineers have focused on developing and using structural lightweight materials. The motivation for mass reduction is directly related to resistance to vehicle performance and fuel consumption and correspondingly automotive emissions. In this endeavor, Mg alloys and composites have received special interest.

The rapid increase in commercial usage of die cast Mg alloys may be attributed almost entirely to automotive use. Apart from being lighter than aluminum other factors that make use of Mg lucrative are its good castability and machinability. Also, low heat capacity and latent heat of solidification are further advantages to Mg resulting in shorter casting cycles and longer die life [1-3].

Understanding of wear behaviour of cast Mg alloys is critical for their use in engine powertrain applications. Piston cylinder bore assemblies, running under lubricated conditions should result in very little material removal, with the wear rate not exceeding a few nanometers per hour [4]. This feature qualifies engine wear to be classified as ultra-mild wear (UMW), since the rate of wear is few orders lower than mild and severe wear and also the micromechanisms of UMW are different. For the hypereutectic Al-Si alloys (e.g., Al-18.5% Si) with large primary Si particles, the surface damage is limited to the tops of these particles, with the alloy retaining its original microstructure. The UMW in eutectic Al-Si alloys is characterized by sinking-in of the Si particles into the matrix. The Si particles with large aspect ratio are usually fractured. The Al matrix suffers damage until a protective oil-residue layer forms comprising of fractured silicon particles comminuted to nano-size fragments and organic components. Once this layer is formed the matrix is protected from further wear and UMW regime prevails as long as the layer remains intact [4-7].

Reinforcing Mg alloys with discontinuous ceramic fibres and particles helps to improve wear resistance. Alahelisten et al. [8] examined Al_2O_3-fibre-reinforced Mg–9Al–1Zn (AZ91) composites in sliding, abrasion and erosion tests. The authors observed that the sliding wear resistance was the highest for an optimum fibre content of 10%. For two body abrasion, abrasion resistance improved continuously with fibre content. Other studies with Mg alloys reinforced with Al_2O_3 fibres, SiC and TiC particles have been reported [9-12]. In all these studies dry sliding wear behaviour of Mg composites was studied at different loads and the general observation was that wear resistance of the composite was considerably higher than that of the unreinforced alloy. However, wear properties of Mg composites under lubricated conditions and at low loads, replicating the actual engine operating conditions, is missing in the literature. In this study a Mg alloy, AM60, reinforced with short discontinuous Al_2O_3fibres was subjected to boundary lubricated sliding wear under UMW conditions. Understanding the wear mechanisms of Mg matrix composites reinforced with Al_2O_3 fibres is expected to facilitate the tribological design of powertrain castings for automotive lightweight strategy.

Experimental Procedure

Materials

The matrix alloy used for this study was squeeze cast Mg alloy AM60 with a composition (wt%) consisting of Al: 5-6%, Mn: 0.4% etc. Short (20.91±5.9 μm) Al_2O_3 fibres (9 vol%) were incorporated in the alloy to form fibre reinforced composites. The composites were prepared by squeeze casting method. Al_2O_3 fibres were made into slurry by adding organic and inorganic binders and later dried and sintered to prepare the preform. Both the upper and the lower dies were preheated to 350 °C. The preform and the alloy were heated to 450 °C and 750 °C before pouring it into the lower die. Once the molten magnesium was added to the die containing the Al_2O_3 fibres, the dies were closed by raising the lower die and fitting into the upper one. In this way the plunger pushed the molten Mg alloy and the preform into the die cavity under a constant pressure of 90 MPa applied by the plunger to allow liquid Mg alloy to infiltrate into the gaps between the Al_2O_3 fibres. This presuure was maintained until the solidification of the casting was complete [12]. The resulting alumina reinforced composite was designated as AM60-9% $(Al_2O_3)_f$. The matrix hardness was 51.0 ± 8.0 HV and the overall hardness of AM60-9% $(Al_2O_3)_f$ was 121.8 ± 11.1 HV. Figure 1 show the setup used to fabricate the composite.

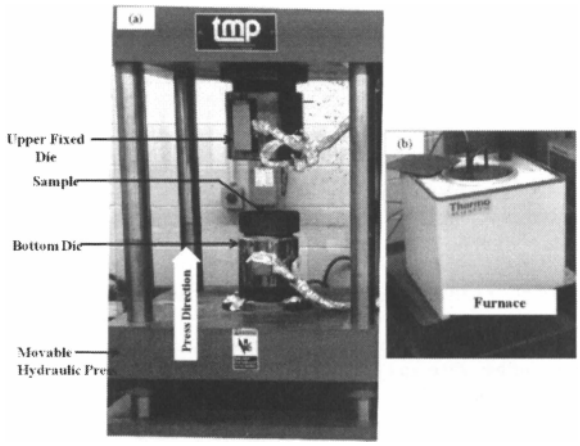

Figure 1 – (a) The squeeze casting machine and (b) the furnace. The dies are closed by raising the lower die against the upper one by the hydraulic press. The magnesium alloy AM60 is melt at 750 °C in the furnace.

Wear Testing

A pin-on-disk type of tribometer was used to perform lubricated sliding wear tests on AM60-9% $(Al_2O_3)_f$ against 6 mm diameter AISI 52100 grade steel balls (848 HV). Sliding wear tests were performed on the composite under 1.0 N, 2.0 N, 5.0 N loads and for sliding cycles between 2.5×10^4-1.0×10^6 at a constant sliding velocity of 0.05 m/s. Wear tests were also performed on the matrix alloy AM60 at 1.0 N load for comparison. All wear tests were conducted at room temperature under boundary lubricated conditions using synthetic oil SAE 5W-30. The lubrication regime was evaluated by calculating the ratio (λ) of minimum lubrication thickness and the root mean square roughness of the surfaces in contact [13] and λ was found to be 0.25, 0.24, 0.22 for 1.0, 2.0, 5.0 N loads respectively. The worn surfaces were analyzed using a scanning electron microscope (JEOL 6400) equipped with an energy dispersive spectrometer (EDS) and were quantified using an optical surface profilometer (WYKO NT 1100).

The wear rate of AM60 alloy was calculated by mass difference method from the volume lost vs. sliding distance plot. Wear of composites occurred in the UMW regime where wear losses were less than that could be measured using mass difference method using a balance with high sensitivity (10^{-5} g). Hence, optical profilometry calculations were employed to determine the material removal rates in the composites according to the reference 4. The amount of material removal associated with the groove formations along the wear track were detected in this way. The amount of material removed was obtained from an area A by calculating the cross-sectional area that fell below a reference position with respect to unworn magnesium matrix. The calculated area (Aij) from eight different portions of the wear multiplied by the perimeter of the wear track gives the volumetric wear loss W according to the equation 1 [4]:

$$W = \frac{2}{n}\pi R_w \left[\sum_{i=1}^{n}\sum_{j=1}^{k} A_{ij}\right] \quad (1)$$

where, k is the number of grooves per section and n=24: number of different sections along the wear track from which measurements were made.

Preceding the wear loss calculated as above was the observation that Al_2O_3 fibres that were initially protruded above the matrix fractured and buried into the matrix during sliding contact. The difference in elevation of the Mg matrix and the Al_2O_3 fibres was quantified by optical profilometry measurements from which histogram showing the distribution (frequency) of Mg matrix and Al_2O_3 fibre was plotted. The second Gaussian peak, with higher frequency represents the Mg matrix. This peak serves as the reference point for the other Gaussian peak which represents the Al_2O_3 fibre elevation with respect to the matrix.

Results and Discussion

Wear of Unreinforced Alloy; AM60

Figure 2 shows the wear losses of AM60 alloy and AM60-9% $(Al_2O_3)_f$ composite plotted as a function of sliding cycles. It is evident that the wear loss from the surface of AM60 alloy was 10^2 times higher than that of AM60-9% $(Al_2O_3)_f$ despite the fact that the wear losses for the composite reported in this figure were measured at 5.0 N load. Figure 3a shows the SEM micrograph of wear track of the AM60 alloy at 1.0 N for 2.5×10^4 sliding cycles and Figure 3b shows the wear track of AM60-9% $(Al_2O_3)_f$ at 2.0 N for 6.0×10^5 sliding cycles. The greater extent of wear (width of wear track: 0.73±0.08 mm) for the AM60 alloy at 1.0 N in comparison to the composite (width of wear track: 0.35±0.02 mm) is evident despite being worn at a higher load and for longer sliding cycles.

Secondary scanning electron micrographs of the worn surfaces of the alloy (Figure 4a and b) revealed the prevalent wear features at higher magnification. For low cycles (i.e., for < 5.0×10^4 cycles), the damage was in the form of surface plastic deformation. At higher sliding cycles, evidence for oxidative wear was found in addition to the matrix surface deformation. Presence of MgO was detected in the form of wear debris on the wear track and also in the material transferred to the counterface. The material removal rate for the AM60 alloy, 5.67×10^{-4} mm^3/m, indicated mild wear throughout the test conditions. According to Fig 2, in the mild wear regime, the volume loss due to sliding wear increased linearly with the sliding distance, indicating that wear progressed under the steady state (i.e. constant wear rate) conditions.

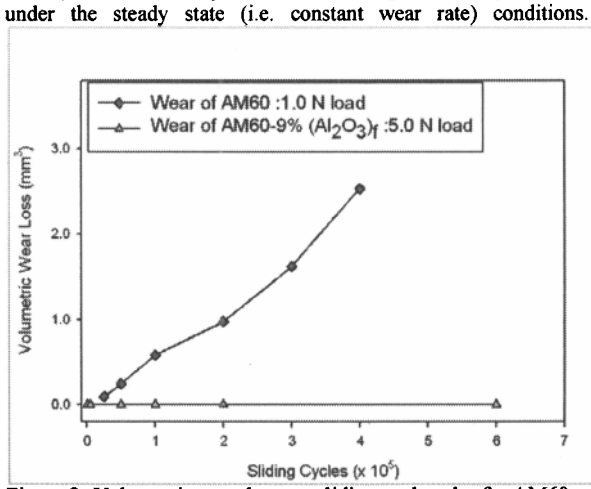

Figure 2- Volumetric wear loss vs. sliding cycles plot for AM60 alloy and AM60-9% $(Al_2O_3)_f$ .The wear loss of the composite is 10^2 times lower than that of the matrix alloy. Note the wear of the composite was shown at 5.0 N and the matrix at 1.0N load.

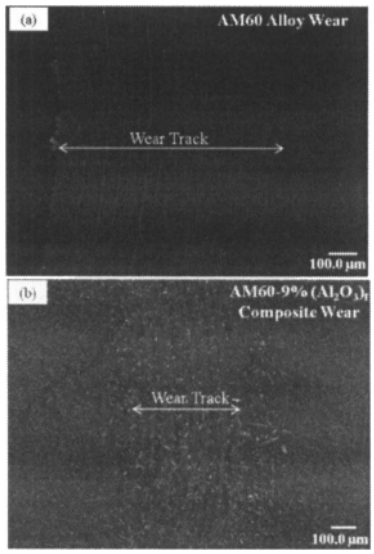

Figure 3- SEM micrographs showing the difference in the width of wear tracks of (a) AM60 alloy at 1.0 N and 2.5×10^4 cycles and (b) AM60-9% $(Al_2O_3)_f$ at 2.0 N and 6×10^5 cycles indicating the wear resistance of the ceramic reinforced composite is higher than the alloy.

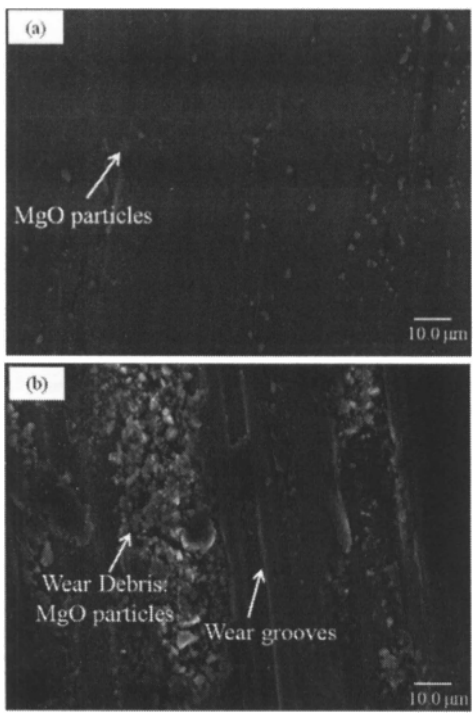

Figure 4- SEM Micrographs showing wear damage of AM60 alloy under 1.0 N load at (a) 2.5×10^4 cycles and (b) 4.0×10^5 cycles. Plastic deformation and oxidative type wear are detected.

Wear of Composite; AM60-9% $(Al_2O_3)_f$

Wear of AM60-9% $(Al_2O_3)_f$ occurred in the UMW regime. Figure 5 indicates the volumetric wear loss against the sliding cycles at three different loads and helps correlate the material removal rates to the wear features at each load when examined together with the SEM images of contact surfaces (Fig 6). Under 1.0 N load Al_2O_3fibres protected the magnesium matrix from damage by counterface for up to the longest sliding cycles (1×10^6) used. Thus, the material removal from the matrix was essentially nil for all sliding cycles (Figure 5). The wear was limited to the tops of the Al_2O_3 fibres. Some fibre fracture and decohesion of fibres from the matrix were also observed.

Similar features were observed at 2.0 N load for up to 2×10^5 sliding cycles. For $\geq 6\times10^5$ cycles wear damage to the matrix surface was observed in the form of wear grooves covering the entire wear track. Consequently, at this point the wear rate increased to 1.35×10^{-7} mm^3/m as shown in Figure 5.

At 5.0 N load the magnesium matrix damage incurred as early as 1×10^5 sliding cycles. The SEM images in Figure 6 show the effects of load on the wear of AM60-9% $(Al_2O_3)_f$: 1.0 N load even for 6.0×10^5 cycles the matrix was unscathed (Figure 6a) whereas at 5.0 N damage to the matrix was observed at 2.0×10^5 cycles (Figure 6b). EDS analysis of the worn surfaces of the AM60-9% $(Al_2O_3)_f$ composites showed presence of iron particles which were transferred from the counterface.

Thus at higher loads and higher sliding cycles, the material removal rate was considerably high and correspondingly the wear rate was found to increase cumulatively (Figure 5). However, the highest wear rate estimated at 5.0 N for 2.0×10^5 cycles was 1.82×10^{-6} mm^3/m which was of the order of 10^2 times lower than that of the AM60 alloy.

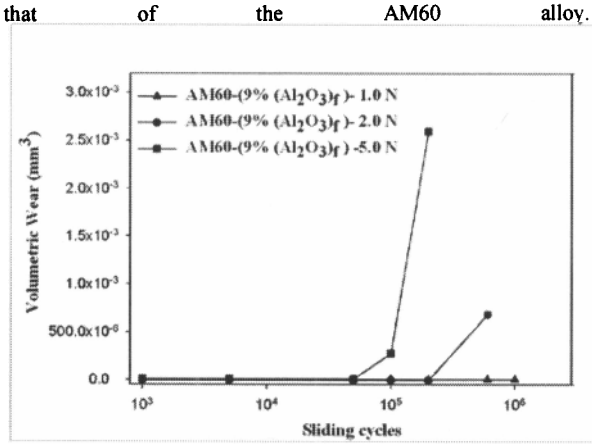

Figure 5- Wear rate for AM60-9% $(Al_2O_3)_f$ composites showing the dependence of wear rate on the applied load and sliding cycles.

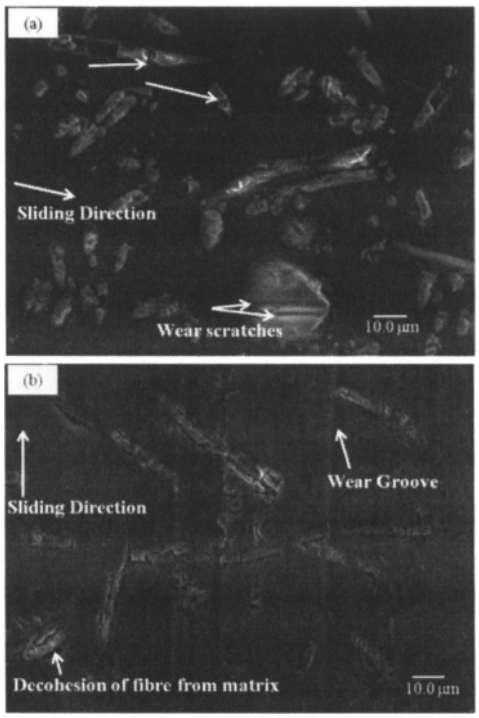

Figure 6-SEM micrographs showing the effect of applied load on the wear of AM60-9% $(Al_2O_3)_f$. (a) At 1.0 N load and 6.0×10^5 cycles the matrix is protected by the alumina fibres; (b) at 5.0 N load and 2.0×10^5 cycles the matrix was plastically deformed by the counterface.

The higher wear resistance of the AM60-9% $(Al_2O_3)_f$ and its wear rate dependence on load may be related to the increase in the strength of the composite. The addition of discontinuous aluminum oxide short fibres to the AM60 alloy increased the yield strength of the composite from 81 to 125 MPa and tensile strength increased from 171 to 182 MPa [12]. However it is more insightful to consider the wear resistance at microscopic level in the following way: As indicated above the Al_2O_3 fibres in the magnesium matrix composite acted as load bearing elements thus protecting the softer matrix from wear by the counterface. Prior to every wear test the sample was finely ground by SiC emery papers to 4000 grit and finally polished by water based diamond suspensions of 3 and 1µm. This process led to an elevation of the Al_2O_3fibres by 1.8 ± 0.2 µm, above the magnesium matrix, as determined by optical profilometry (Figure 7). Thus, the AISI 52100 counterface slides against the elevated alumina fibres leaving the softer matrix untouched. As the sliding cycles and applied load was increased the Al_2O_3 fibres fractured and the fractured fragments were embedded into the magnesium matrix until the fibres and the matrix came to the same elevation (Figure 7). At this point sliding by the counterface on the soft magnesium matrix caused wear grooves on the wear track. This was reflected in the wear rate plot for the composites (Figure 5). As shown by the change of the slopes of the wear curves in figure 5, the sliding cycles at which the matrix damage initiates becomes shorter with increasing the applied load. However, it should be noted that despite the increase in slope the wear rates remain sufficiently low for all applied sliding cycles so that wear of AM60-9% $(Al_2O_3)_f$ remains in UMW regime. The wear behaviour of AM60-9% $(Al_2O_3)_f$ at higher cycles should be further examined to determine if a transition to higher wear regime would occur.

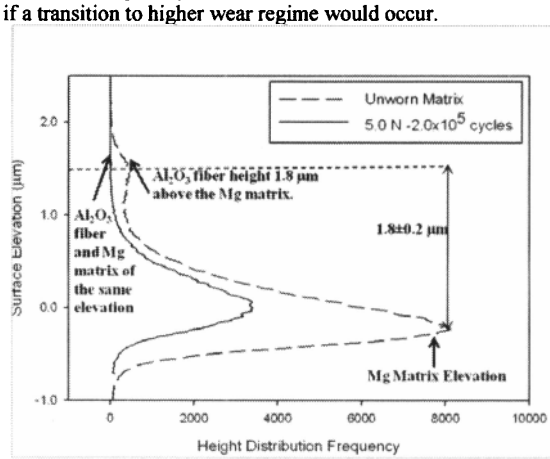

Figure 7- Histogram showing the height differences between the magnesium matrix and the alumina fibres for the unworn surface and also the worn surface after 2×10^5 cycles at 5.0 N load. For the unworn surface the average height difference is 1.8 µm whereas for the worn surface the height of the matrix and the fibres are the same after 2×10^5 cycles at 5.0 N load.

Wear of Counterface; AISI 52100

When AISI 52100 counterface was worn against the matrix alloy AM60 the wear on the surface of the counterface was limited to the formation of scratch marks (Figure 8a). EDS analysis of the counterface showed presence of transferred magnesium oxide wear debris, which indicated oxidative type wear between the steel ball and the magnesium alloy.

In AM60-9% $(Al_2O_3)_f$ composite-counterface system, initial contact always occurred between the Al_2O_3 fibres and the AISI 52100 surface. Since the ceramic fibres were harder (1365 HV) than the steel (848 HV), wear groove formation was detected on AISI 52100 (Figure 8b). EDS analysis of the counterface indicated no material transfer between the composite and the counterface. Presence of Fe particles was detected on the wear track of the composite which probably resulted from the transfer of material from the counterface (Figure 9). Thus Al_2O_3 fibres in AM60-9% $(Al_2O_3)_f$ composite proved to be disadvantageous for the wear of the counterface AISI 52100

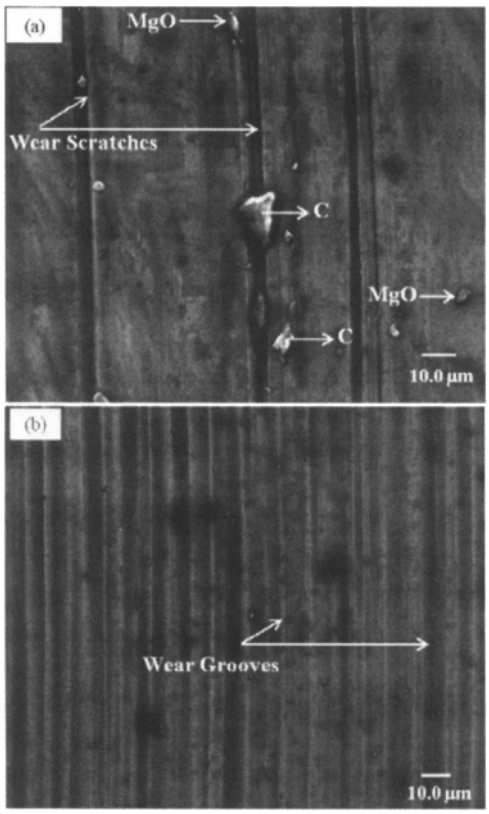

Figure 8- SEM micrograph showing the worn surface features of the counterface due to wear against (a) AM60 alloy at 1.0 N and 2.5×10^4 cycles and (b) AM60-9% $(Al_2O_3)_f$ at 1.0 N and 2.0×10^5 cycles. Transfer of wear debris (MgO) from the alloy to the counterface was detected.

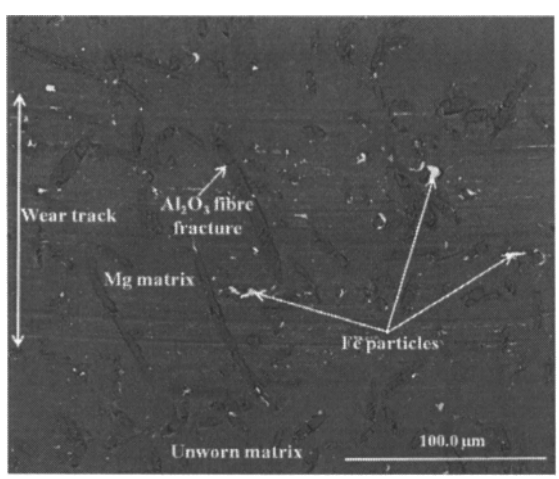

Figure 9- Back-scattered micrograph of worn surface of AM60-9% $(Al_2O_3)_f$ at 5.0 N and 1.0×10^5 cycles showing presence of iron particles transferred from the counterface AISI 52100 due to sliding against harder alumina fibres.

Summary and Conclusions

Magnesium alloy AM60 incorporating short discontinuous Al_2O_3 fibres prepared from a perform were used to fabricate an AM60-9% $(Al_2O_3)_f$ composite by squeeze casting method. The matrix alloy and the composite were subjected to boundary lubricated sliding wear under 1.0-5.0 N load. The main findings of the study are summarized as follows:

1. Wear mechanisms of magnesium alloy, AM60, at 1.0 N consisted of damage by surface plastic deformation and oxidative type wear. Material removal rate for the AM60 alloy, 5.67×10^{-4} mm^3/m, indicated occurrence of mild wear throughout test conditions. Formation of wear debris, consisting of MgO particles, was observed on the wear track after 4×10^5 sliding cycles. Transfer of magnesium oxide particles from the alloy to the counterface was detected.
2. Wear of AM60-9% $(Al_2O_3)_f$ composite under 1.0-5.0 N loads occurred in ultramild wear regime, with wear rates $< 2.0\times10^{-6}$ mm^3/m. With increase of applied load and sliding cycles, there was an increase in rate of Mg matrix removal.
3. The Al_2O_3 fibres protected the matrix from damage by the counterface up to a certain sliding distance, which decreased with the increase in the applied load. Fibre fracture and interfacial decohesion led to the embeddeing of the fibres into the matrix and eventually resulting in an increased rate of material removal.
4. Wear of the counterface, AISI 52100, during sliding against the magnesium alloy AM60, was low and manifested in the form of wear scratches. The amount of material removal from the counterface was higher when tested against the composite.

It can be concluded that the AM60-9% $(Al_2O_3)_f$ composites possess enhanced wear resistance over the base alloy AM60. However, the greater amount of wear of the counterface at higher loads necessitates further study with respect to modification of the counterface material to reduce the amount of wear therein.

References

1. H. Hu, A. Yu, N. Li and J. Allison, Potential magnesium alloys for high temperature die cast automotive applications: A review, *Materials and Manufacturing Processes*, 18 (2003), 687-717.
2. M. O. Pekguleryuz and A. A. Kaya, Creep resistant magnesium alloys for powertrain applications, *Advanced Engineering Materials*, 5(2003), 866-871.
3. K.M. Asl, A. Masoudi and F. Khomamizadeh, The effect of different rare earth elements content on microstructure, Mechanical and Wear Behavior of Mg-Al-Zn Alloy, *Material Science and EngineeringA*, 527,(2010), 2027-2035.
4. M. Chen, X. Meng-Burany , T.A. Perry and A.T. Alpas, Micromechanisms and mechanics of ultra-mild wear in Al–Si alloys, *Acta Materialia*, 56 (19), (2008), 5605–5616.
5. M. Chen, T.A. Perry and A.T. Alpas, Ultra-mild wear in eutectic Al–Si alloys, *Wear*, 263(2007),. 552–561.
6. M. Chen and A.T. Alpas, Ultra-mild wear of a hypereutectic Al–18.5 wt.% Si alloy, *Wear*, 265 (1–2) (2008), 186–195.
7. S.K. Dey, T.A. Perry, A.T. Alpas, Micromechanisms of low load wear in an Al-18.5% Si alloy, *Wear*, 267 (2009), 515–524.
8. A. Alahelisten, F. Bergman, M. Olsson, and S. Hogmark, On the wear of aluminium and magnesium metal matrix composites, *Wear*, 165 (1993), 221-226.

9. B. Hu, L. Peng and W. Ding, Dry sliding wear behavior of Saffil fiber-reinforced Mg-10Gd-3Y-0.5Zr magnesium alloy-based composites, *Journal of Composite Materials*, 45(201), 683–693.
10. C.Y.H. Lim, S.C. Lim and M. Gupta, Wear behaviour of SiCp-reinforced magnesium matrix composites, *Wear*, 255(2003), 629–637.
11. S.J. Huang, Y.R Jeng., V. I. Semenov and Y.Z. Dai, Particle Size Effects of Silicon Carbide on Wear Behavior of SiCp-Reinforced Magnesium Matrix Composites, *Tribological Letters*, 42(2011), 79–87.
12. L.F. Franco, E. B. Becerril, J. L. Ruiz, J.G. Gonzalez-Rodriguez, R. Guardian and I.Rosales, Wear performance of TiC as reinforcement of a magnesium alloy matrix composite, *Composites:Part B*, 42(2011), 275-279.
13. Q. Zhang and H. Hu, Advances in Light Weight Materials– Aluminum, Casting Materials and Magnesium Technologies, *SAE 2010 World Congress*, (2010), 107-114.
14. I.M. Hutchings, Tribology: Friction and Wear of Engineering Materials-(Metallurgy & Materials science series), (CRC Press, 621.89, 1992), 77-105.